Preprints of the 19th World Congress
The International Federation of Automatic Control
Cape Town, South Africa. August 24-29, 2014

Autonomous Rendezvous Control and Determination of Unknown Target Orbit ⋆

Lijia Xu * **Yong Hu** * **Tiantian Jiang** *

* *Science and Technology on Space Intelligent Control Laboratory, Beijing Institute of Control Engineering, 100190 Beijing, P.R.China (e-mail: predest@sina.com).*

Abstract: This paper studies the space rendezvous problem with the target spacecraft in an unknown elliptical orbit. By the measurements of the relative position and velocity between the chaser spacecraft and the target spacecraft, a control strategy is proposed to achieve autonomous rendezvous. In addition, the orbital information can be estimated in the rendezvous process, and then the orbital elements are calculated by the estimate information. Finally, the proposed approach is illustrated by simulations.

Keywords: Autonomous Rendezvous, Elliptical Orbit, Orbit Control, Orbit Determination, Parameter Estimation.

1. INTRODUCTION

Autonomous rendezvous and docking have become an important trend for future space missions, which will bring many benefits, such as reduction of costs, improved flexibility of the space task, and so on.

The related work of this issues has added insights into the rendezvous or formation control (Wong et al. (2002); Inalhan et al. (2002)) with the target in an arbitrary elliptical orbit. In this case, the relative motion dynamics are nonlinear and with time-varying parameters which are the functions of the orbital elements. In previous work, the target orbital elements are considered as priori knowledge and the chaser spacecraft is able to receive real-time information by communication with the target spacecraft or ground stations. One method is to compensate the nonlinear terms with time-varying parameters by designing feedback control with known orbital information, such as Singla et al. (2006), Karlgaard and Schaub (2011), and Singla and Subbarao (2008). Another method (Zhou et al. (2011); Gao et al. (2012)) is to design control law based on the simplified relative motion equations by using the true anomaly of the target spacecraft as an independent variable instead of time (Yamanaka and Ankersen (2002)). The initial orbital information also needs to be known.

However, the above-mentioned methods are obviously not feasible for unknown and non-cooperative targets such as damaged spacecrafts or space debris with no communication between them. To address this issue, Lu and Xu (2009) develop a control strategy for the spacecraft autonomous rendezvous and it is achieved that the final relative position and velocity are bounded. Furthermore, it is worth mentioning that Characteristic Modeling (Wu et al. (2007)) for this uncertain system is a very effective method, the intelligent adaptive control based on the characteristic model can meet the engineering requirements and has been applied in the rendezvous and docking control for Shenzhou spacecraft (Xie et al. (2013)). However, the common deficiency is that the target orbital information can not be obtained which may be key information for other space missions. To the authors' best knowledge, there are no related methods have been proposed for control of autonomous rendezvous while the target orbital elements are estimated by the relative position and velocity in the rendezvous process.

In this paper, we consider the problem of autonomous rendezvous with the target spacecraft in an unknown elliptical orbit. The main work can be divided into two parts. One is control design for autonomous rendezvous. Since the out-of-plane and in-plane motions can be seen as decoupled, control laws are designed respectively to track the reference trajectories. A brief stability analysis is given. The second is determination of the unknown target orbit. During approaching, orbital information can be estimated by measurements. Orbital elements can be calculated from the estimate information directly. Finally, a numerical example is given to show the effectiveness of the proposed methodology.

2. PROXIMITY RELATIVE MOTION

In this section, the proximity model we use for the relative motion control is set forth.

2.1 Coordinate System

The target-orbital coordinate system is introduced to establish the relative motion between the target spacecraft and the chaser spacecraft.

⋆ The work was supported by the National Key Basic Research and Development Program under Grant 2013CB733100, the National Natural Science Foundation of China under Grant 61333008 and 61304027, and the Creative Foundation of China Academy of Space Technology (CAST).

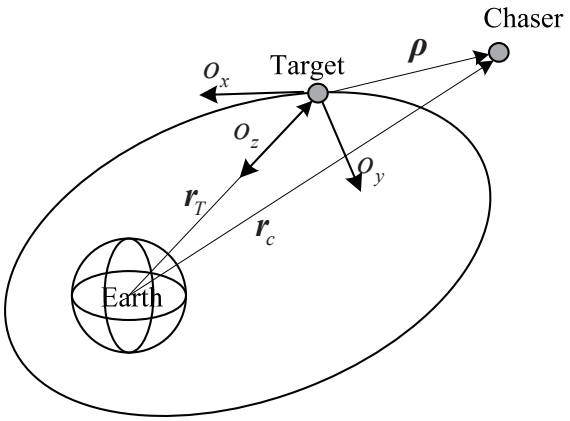

Fig. 1. Coordinate for the relative motion

The target-orbital reference frame is attached to the center of mass of the target spacecraft. O_x-axis and O_z-axis are inside the orbital plane, O_z-axis is oriented toward the center of the planet, O_x-axis points forward and is perpendicular to O_z-axis. O_y-axis is normal to the orbital plane, completing the right-handed system. The frame is illustrated in Fig. 1, $\boldsymbol{r}_T$, $\boldsymbol{r}_c$ are the vectors from the center of gravity to the target spacecraft and chaser spacecraft, and $\boldsymbol{\rho}$ is the vector from the target spacecraft to the chaser spacecraft.

2.2 Relative Motion Dynamic

The target spacecraft is in an arbitrary elliptical orbit. It is assumed that the distance between the chaser spacecraft and the target spacecraft is much smaller than the distance between the target spacecraft and the center of the planet. Then, the chaser motion relative to the target spacecraft in the target-orbital coordinate system can be described as the well-known TH equations (Yamanaka and Ankersen (2002))

$$\begin{aligned} &\ddot{x} - 2\dot{\theta}\dot{z} - \ddot{\theta}z - \dot{\theta}^2 x + k\dot{\theta}^{3/2}x = u_x \\ &\ddot{y} + k\dot{\theta}^{3/2}y = u_y \\ &\ddot{z} + 2\dot{\theta}\dot{x} + \ddot{\theta}x - \dot{\theta}^2 z - 2k\dot{\theta}^{3/2}z = u_z \end{aligned} \tag{1}$$

where x, y, and z represent the relative positions of the chaser spacecraft with respect to the target spacecraft, $k = \frac{\mu}{h^{3/2}} = \frac{\mu^{1/4}}{[a(1-e^2)]^{3/4}}$ is a defined constant, μ is the gravity constant, h is the orbital angular momentum of the target orbit, a and e are the semimajor axis and eccentricity of the target orbit, $\dot{\theta}$ and $\ddot{\theta}$ are, respectively, the orbital angular velocity and angular acceleration of the target spacecraft. The explicit expressions of them will be explained next.

2.3 Orbital Information in Equations

The time-varying parameters in (1), i.e., $\dot{\theta}$, $\ddot{\theta}$, $\dot{\theta}^2$, and $k\dot{\theta}^{2/3}$, are given in this subsection.

The Kepler's equation is

$$E - e\sin E = \sqrt{\frac{\mu}{a^3}}(t - t_p) \tag{2}$$

where t_p renders the time of perigee passage, t is a current time, and E is the eccentric anomaly. The equations about E and the true anomaly θ satisfy

$$\sin\theta = \frac{\sqrt{1-e^2}\sin E}{1 - e\cos E}, \qquad \cos\theta = \frac{\cos E - e}{1 - e\cos E}, \tag{3}$$

and the expressions of $\dot{\theta}$ and $\ddot{\theta}$ satisfy the following equations

$$\dot{\theta} = k^2(1 + e\cos\theta)^2, \tag{4}$$

$$\ddot{\theta} = -2k^4 e\sin\theta(1 + e\cos\theta)^3, \tag{5}$$

$$\dot{\theta}^2 = k^4(1 + e\cos\theta)^4, \tag{6}$$

$$k\dot{\theta}^{3/2} = k^4(1 + e\cos\theta)^3. \tag{7}$$

From (2)-(7), it can be observed that the four time-varying parameters $\dot{\theta}$, $\ddot{\theta}$, $\dot{\theta}^2$, and $k\dot{\theta}^{2/3}$ are determined by three orbital elements a, e, and t_p, which are the main orbital influencing factors for autonomous rendezvous. Therefore, the further developments contained in this paper will focus on control for rendezvous and estimation of the three orbital elements.

3. RENDEZVOUS CONTROL

In this section, we develop control laws for autonomous rendezvous.

It is noted that the out-of-plane motion (i.e., the O_y-axis subsystem) and the in-plane motion (i.e., the O_x - O_z-axis subsystem) are independent. Therefore, they can be considered separately. For out-of-plane and in-plane motion, we design different control laws to track designed reference trajectories. The common target is to achieve autonomous rendezvous and pave the way for estimation of the orbital elements. Details are shown in the following subsections.

3.1 Generation of Reference Trajectories

We first introduce an approach to generate the reference trajectories.

To achieve autonomous rendezvous, a pre-designed reference trajectory for translation motion needs to take initial relative position and velocity, and the final anticipated relative position and velocity into account. Moreover, the trajectory should be smoothly and available to be tracked under the limitation of the control ability. Here, we adopt Bézier polynomial (Westervelt et al. (2007)), that is

$$r(s) = \sum_{k=0}^{M} \alpha_k \frac{M!}{k!\,(M-k)!} s^k (1-s)^{M-k} \tag{8}$$

where $r(s) : [0,1] \to \mathbb{R}$, M is the degree of the polynomial, and α_k can be selected by boundary conditions and all kinds of constraints.

Translate variable s into time t by

$$s = \frac{t - t_0}{t_f - t_0} \tag{9}$$

where t_0 and t_f are the initial and final time of rendezvous. Then, we can get the reference trajectory of O_x-axis

$$x_r = r(s), \quad \dot{x}_r = \frac{dr}{ds}\dot{s}, \quad \ddot{x}_r = \frac{d^2r}{ds^2}\dot{s}^2. \tag{10}$$

The reference trajectories for O_y-axis and O_z-axis can be generated in the same way.

Next, we will present the control laws for out-of-plane motion and in-plane motion.

3.2 Control Design for Out-of-plane Motion

The out-of-plane motion is simple and the estimate of $k\dot{\theta}^{3/2}$ has an impact on the control design for in-plane motion, so we consider it first.

Out-of-plane motion equation in (1) is

$$\ddot{y} + k\dot{\theta}^{3/2} y = u_y. \tag{11}$$

We define $w_0(t) = k\dot{\theta}^{3/2}$, then (11) becomes

$$\ddot{y} = -w_0(t)y + u_y \tag{12}$$

where $w_0(t)$ is a time-varying parameter. Next, we will design a trajectory tracking control law and a time-varying parameter estimation method.

The estimation of the time-varying parameter $w_0(t)$ is carried out by derivation-free weight update law (Yucelen and Calise (2011))

$$\hat{w}_0(t) = r_1 \hat{w}_0(t - \tau) + \hat{q}(t) \tag{13}$$

where $\hat{w}_0(t)$ is an estimate of $w_0(t)$, $0 \le r_1 < 1$, $\tau > 0$, and $\hat{q}(t)$ satisfies

$$\hat{q}(t) = r_2 E_y^T P_y B_y y \tag{14}$$

where $r_2 > 0$, $B_y = [\,0\ 1\,]^T$, $E_y = [\,e_y\ \dot{e}_y\,]^T$, $e_y = y - y_r$ is the tracking error, y_r is the reference trajectory which has been given in the last subsection, and $P_y \in \mathrm{R}^{2\times 2}$ is the positive-definite solution of the Lyapunov equation

$$A_y^T P_y + P_y A_y + Q_y = 0 \tag{15}$$

where $Q_y = Q_y^T > 0$, $A_y = \begin{bmatrix} 0 & 1 \\ -k_{1y} & -k_{2y} \end{bmatrix}^T$, and $k_{1y}, k_{2y} > 0$.

Then, the control law for the out-of-plane motion is designed as

$$u_y = \ddot{y}_r - k_{1y} e_y - k_{2y} \dot{e}_y + \hat{w}_0(t) y. \tag{16}$$

Remark 1. The form in (13) and (14) can estimate the time-varying parameter $w_0(t)$. It uses the information of delayed weight estimate $w_0(t - \tau)$, the current position information y, and trajectory tracking errors E_y. Detailed analysis about the estimation ability and closed-loop stability are in the section of stability analysis.

3.3 Control Design for In-plane Motion

In this subsection, we introduce the control design for in-plane motion.

Since the relative motion is coupled in O_x-axis and O_z-axis, a decoupling method will be introduced. We treat the system states, time-varying parameters, and other terms as an extended state, then, the extended state observer (ESO) (Han (2009)) is used to estimate the extended state. In particular, the estimated extended state will be used in the orbit determination later.

The motion of O_x-axis in (1) is

$$\ddot{x} = 2\dot{\theta}\dot{z} + \ddot{\theta} z + \dot{\theta}^2 x - k\dot{\theta}^{3/2} x + u_x. \tag{17}$$

Denote $\varphi_x(t) = 2\dot{\theta}\dot{z} + \ddot{\theta} z + \dot{\theta}^2 x$, $u_x' = u_x - \hat{w}_0(t)x$, and weight update error $\tilde{w}_0(t) = w_0(t) - \hat{w}_0(t)$, then (17) becomes

$$\ddot{x} = \varphi_x(t) - \tilde{w}_0(t)x + u_x'. \tag{18}$$

We define $x_1 = x$, $x_2 = \dot{x}$, and $x_3 = \varphi_x(t) - \tilde{w}_0(t)x$, then (18) can be rewritten as

$$\begin{aligned} \dot{x}_1 &= x_2 \\ \dot{x}_2 &= x_3 + u_x'. \end{aligned} \tag{19}$$

Since the relative position x and relative velocity $\dot{x}$ are available for measurement, we adopt a reduced order ESO, that is

$$\begin{aligned} \dot{x}_0 &= -\beta_x x_0 - \beta_x^2 x_2 - \beta_x u_x' \\ \hat{x}_3 &= x_0 + \beta_x x_2 \end{aligned} \tag{20}$$

where $\hat{x}_3$ is the estimate of x_3, x_0 is a state of ESO, and β_x is a high-gain value. In general, we set $\beta_x = \frac{\bar{\beta}_x}{\epsilon}$, where $\bar{\beta}_x$ is a positive constant, and ϵ is a small and positive constant.

Then, the control law for (17) is designed as

$$u_x = \ddot{x}_r - k_{1x} e_x - k_{2x} \dot{e}_x + \hat{w}_0(t) x - \hat{x}_3 \tag{21}$$

where $k_{1x}, k_{2x} > 0$.

Similarly, consider the O_z-axis motion in (1)

$$\ddot{z} = -2\dot{\theta}\dot{x} - \ddot{\theta} x + \dot{\theta}^2 z + 2k\dot{\theta}^{3/2} z + u_z \tag{22}$$

and design control law for O_z-axis as

$$u_z = \ddot{z}_r - k_{1z} e_z - k_{2z} \dot{e}_z - 2\hat{w}_0(t) z - \hat{z}_3 \tag{23}$$

where $k_{1z}, k_{2z} > 0$, $\hat{z}_3$ is the estimate of the extended state z_3, which is defined as $z_3 = -2\dot{\theta}\dot{x} - \ddot{\theta} x + \dot{\theta}^2 z + 2\tilde{w}_0(t) z$. The extended state z_3 is estimated by the reduced order ESO

$$\begin{aligned} \dot{z}_0 &= -\beta_z z_0 - \beta_z^2 z_2 - \beta_z u_z' \\ \hat{z}_3 &= z_0 + \beta_z z_2 \end{aligned} \tag{24}$$

where $u_z' = u_z + 2\hat{w}_0(t) z$, and the symbols z_0, z_2, and β_z have the similar definitions of x_0, x_2, and β_x in ESO of O_x-axis.

3.4 Stability Analysis

In this subsection, we show the stability of the closed-loop system under the control laws mentioned above.

Theorem 1. Consider the rendezvous motion system given by (1), the control laws given by (16), (21), and (23) with the parameter and state estimation components given by (13),(14), (20), and (24). Then, the estimate errors ($\tilde{w}_0(t)$, $\tilde{x}_3(t)$, and $\tilde{z}_3(t)$) and the tracking errors ($E_y(t)$, $E_x(t)$, and $E_z(t)$) are ultimately bounded.

Proof. Here, we give a brief proof of the theorem.

First, we analyze the out-of-plane subsystem.

We consider the following Lyapunov-Krasovskii function

$$V_y(E_y, \tilde{w}(t)) = E_y^T P_y E_y + \lambda \int_{t-\tau}^{t} \tilde{w}_0^2(\varsigma) d\varsigma \tag{25}$$

where $\lambda > 0$. Based on the analysis by Yucelen and Calise (2011), we can obtain that the tracking error $E_y(t)$ and the weight update error $\tilde{w}_0(t)$ are ultimately bounded. The error trajectory approaches the ultimate bound exponentially in time. Therefore, there exists constants $t_y > 0$, $\epsilon_y > 0$, and $\delta_y > 0$, such that $t \geq t_y$, then $\| E_y(t) \| \leq \epsilon_y$ and $|\tilde{w}_0(t)| \leq \delta_y$.

Then, we consider the in-plane subsystem.

By (17)-(21), we can write the closed-loop system of O_x-axis

$$\begin{aligned} \dot{E}_x &= A_x E_x + B_x \tilde{x}_3 \\ \dot{\tilde{x}}_3 &= -\beta_x \tilde{x}_3 + \dot{x}_3 \end{aligned} \tag{26}$$

where $E_x = [\, e_x \;\; \dot{e}_x \,]^T$, $A_x = \begin{bmatrix} 0 & 1 \\ -k_{1x} & -k_{2x} \end{bmatrix}$, and $B_x = [\, 0 \;\; 1 \,]^T$.

According to previous work on the analysis of ESO by Xue and Huang (2011) and Hang and Guo (2012), we can get similar properties of ESO. Defining a compact region

$$\Omega = \{\, (\xi, \tilde{x}_3) |\, \|\xi\| \leq \rho, |\tilde{x}_3| \leq \gamma_x(\rho) \}$$

where $\xi = [\, x \;\; \dot{x} \;\; y \;\; \dot{y} \;\; z \;\; \dot{z} \,]^T$ is the system state, ρ is a positive number, and $\gamma_x(\rho)$ is a known finite increasing function with respect to ρ. It can be proved that the state trajectory of the closed-loop system can not reach the boundary of Ω.

Furthermore, when $t \geq t_x$ ($t_x > 0$), $|\tilde{x}_3| \leq \delta_x$, $\delta_x = O(\epsilon)$ is the infinitesimal of higher order about ϵ.

Next, we will calculate the bound of the tracking error.

Note that A_x is Hurwitz when $k_{1x} > 0$ and $k_{2x} > 0$. There exist positive matrix P_x and positive constants c_{1x}, c_{2x}, such that

$$A_x^T P_x + P_x A_x = -I, \;\; c_{1x} I \leq P_x \leq c_{2x} I \tag{27}$$

where I is the identity matrix.

Define the following Lyapunov function

$$V_x(E_x) = E_x^T P_x E_x. \tag{28}$$

Derivation of (28) is

$$\begin{aligned} \dot{V}_x(t) &= -E_x^T E_x + 2\tilde{x}_3 B_x^T P_x E_x \\ &\leq -\|E_x\|^2 + 2\,|\tilde{x}_3|\,\|P_x\|\,\|E_x\| \\ &\leq -\|E_x\|^2 + (r\|E_x\|^2 + \frac{c_{2x}^2}{r}\,|\tilde{x}_3|^2) \\ &= -(1-r)\|E_x\|^2 + \frac{c_{2x}^2 \delta_x^2}{r} \\ &\leq -\frac{1-r}{c_{2x}} V_x(t) + \frac{c_{2x}^2 \delta_x^2}{r} \end{aligned} \tag{29}$$

where $0 < r < 1$.

According to the Comparison Principle (Khalil (2002)), we have

$$V_x(t) \leq e^{-\frac{(1-r)}{c_{2x}}(t-t_x)} V_x(t_x) + \frac{c_{2x}^3 \delta_x^2}{r(1-r)}. \tag{30}$$

Obviously, $E_x(t)$ is ultimately bounded, and using $\|E_x\|^2 \leq \frac{V_x}{c_{1x}}$, we get the ultimate bound of E_x is $\epsilon_x = \frac{c_{2x}^{3/2}\delta_x}{\sqrt{r(1-r)c_{1x}}}$.

For O_z-axis subsystem, we have the similar results. That is, the estimate error $|\tilde{z}_3| \leq \delta_z$ when $t \geq t_z$ ($t_z > 0$), and the ultimate tracking error $\|E_z\| \leq \epsilon_z$, where δ_z and ϵ_z are small positive constants.

Hence, it can be concluded that the estimate errors and tracking errors are ultimately bounded.

4. ORBITAL ELEMENTS ESTIMATION

In this section, we present the estimation method for the unknown time-varying parameters in (1) except $k\dot{\theta}^{3/2}$, i.e., $\dot{\theta}$, $\ddot{\theta}$, and $\dot{\theta}^2$, and calculate the orbital elements from the estimate data.

4.1 Parameters Estimation

Up to now, we have obtained the estimate parameter $\hat{w}_0(t)$ from (13) and (14), and the estimated extended states $\hat{x}_3$ and $\hat{z}_3$ from (20) and (24).

In order to improve the estimation precision, we set the start time $t_s \geq \max\{t_x, t_y, t_z\}$.

Next, we will utilize nonlinear Kalman filter to estimate the time-varying parameters.

Define the time-varying parameters in (1)

$$w_1(t) = \dot{\theta}, \;\; w_2(t) = \ddot{\theta}, \;\; w_3(t) = \dot{\theta}^2, \tag{31}$$

then, (31) can be expressed as the nonlinear state equations

$$\begin{aligned} \dot{W}(t) &= F[W(t), t] + \nu \\ \Phi &= \Psi W(t) + \upsilon \end{aligned} \tag{32}$$

where $W(t) = [\, w_1(t) \;\; w_2(t) \;\; w_3(t) \,]^T$ is the state vector of the equations, $\Psi = \begin{bmatrix} 2\dot{z} & z & x \\ -2\dot{x} & -x & z \end{bmatrix}$ is the parameter matrix of the equations, $F[W(t), t] = \begin{bmatrix} 0 & 1 & 0 \\ 0 & 0 & 0 \\ 2w_1(t)w_2(t) & 0 & 0 \end{bmatrix}$ is the nonlinear function matrix about the states of the equations, $\Phi = [\, \hat{x}_3 \;\; \hat{z}_3 \,]^T$ is the measurement value vector

of the equations, $\nu = [\,\nu_1\ \nu_2\ \nu_3\,]^T$ and $\upsilon = [\,\upsilon_1\ \upsilon_2\,]^T$ are treated as zero-mean continuous-time white noise vectors since the estimate errors are much smaller than the states, which are denoted as

$$\nu \sim (0, Q_w), \upsilon \sim (0, R_w)$$

where the covariance matrices Q_w and R_w can be given appropriate values according to the bound of estimate error above-mentioned.

Linearize and get the Jacobi matrix of $F[W(t), t]$

$$\frac{\partial F[W(t),t]}{\partial W(t)} = \begin{bmatrix} 0 & 1 & 0 \\ 0 & 0 & 0 \\ 2w_2(t) & 2w_1(t) & 0 \end{bmatrix}, \tag{33}$$

then the continuous-time extended Kalman filter equations (Simon (2006)) are

$$\begin{aligned} &\dot{\hat{W}}(t) = F[\hat{W}(t), t] + K(t)[\Phi - \Psi\hat{W}(t)] \\ &K(t) = P(t)\Psi^T r_w^{-1}(t) \\ &\dot{P}(t) = \left.\frac{\partial F[W(t),t]}{\partial W(t)}\right|_{W(t)=\hat{W}(t)} \cdot P(t) \\ &+P(t) \cdot \left.\frac{\partial F^T[W(t),t]}{\partial W(t)}\right|_{W(t)=\hat{W}(t)} \\ &-P(t)\Psi^T r_w^{-1}(t)\Psi P(t) + q_w(t) \end{aligned} \tag{34}$$

where $\hat{W}(t)$ is the estimate of $W(t)$.

Remark 2. The continuous-time Kalman filter is proposed to illustrate the effectiveness for the estimation of the time-varying parameters. In practice, we can use the discrete-time Kalman filter instead of the continuous-time one.

4.2 Orbit Determination

In this subsection, we can use those estimate parameters to calculate orbital elements and finally determinate the target orbit.

So far, the four time-varying parameters $w_0(t)$, $w_1(t)$, $w_2(t)$, and $w_3(t)$ all have been estimated. By the analysis in subsection 2.3 , we know that they are the functions of the three orbital elements a, e, and t_p. Therefore, we can use the estimate parameters to find out the three orbital elements.

There are various kinds of data processing methods can be used to deal with it, such as Levenberg-Marguardt, Quasi-Newton, Conjugate-Gradient, etc. Obviously, it's not a difficult problem to obtain the orbital elements from the known estimate parameters. Therefore, the paper here will not show specific steps to achieve that. But in the numerical simulations, the orbital elements a, e and t_p will be calculated to complete the whole simulation.

5. NUMERICAL SIMULATIONS

The rendezvous control laws and orbit determination method in this paper are illustrated in this section by simulations of a particular rendezvous mission.

The unknown initial orbital elements of the target spacecraft are listed in table 1.

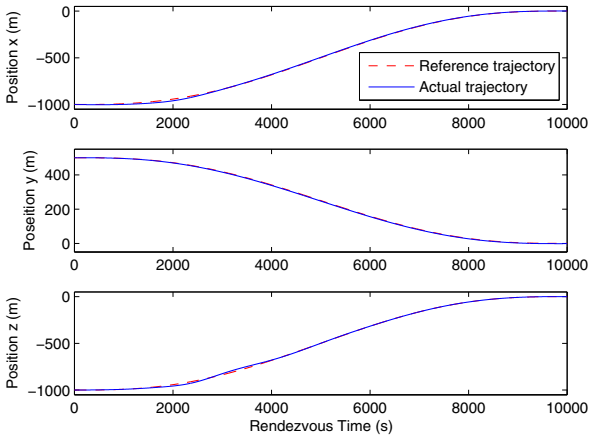

Fig. 2. Position tracking curves

Then, the time of perigee passage t_p can be calculated, which is equal to 2022s.

Furthermore, it is assumed that the chaser spacecraft is at a distance of

$$[\,x(0)\ y(0)\ z(0)\,] = [\,-1000\text{m}\ 500\text{m}\ -1000\text{m}\,]$$

from the target spacecraft, and the initial relative velocity is

$$[\,\dot{x}(0)\ \dot{y}(0)\ \dot{z}(0)\,] = [\,0\text{m/s}\ 0\text{m/s}\ 0\text{m/s}\,].$$

The anticipated final relative position and velocity are all equal to 0, and the rendezvous time is assumed to be 10000s.

Once the relative motion has been established between the two spacecrafts, the reference trajectories can be generated by Bézier polynomial (Subsection 3.1).

Under the proposed control laws (16), (21) and (23), the position tracking curves x, y, z are shown in Fig. 2. As we expected, the chaser spacecraft approaches the target spacecraft along the reference trajectories, and the final position errors are less than 0.5 m, the relative velocity errors are less than 0.1 m/s. The control signals u_x, u_y, u_z of the chaser spacecraft are shown in Fig. 3, which is 10^{-3}m/s^2 order of magnitude.

During the process of rendezvous, the four time-varying parameters, i.e., $w_0(t)$, $w_1(t)$, $w_2(t)$, and $w_3(t)$, can be estimated by (13), (14), (20), (24) and (34). The estimate curves are shown in Fig. 4, and the estimation precisions satisfy the theoretical analysis results.

Based on the above estimate data and functional relations, the orbital elements a, e, and t_p can be calculated by data processing methods. The calculated orbital elements are listed in table 2 which are very close to the true

Table 1. Target orbital elements

Orbital elements	Value
Eccentricity	0.7
Semimajor (km)	22926
Initial true anomaly (deg)	-100
Inclination (deg)	30
Longitude of the ascending node (deg)	0
Argument of perigee (deg)	0

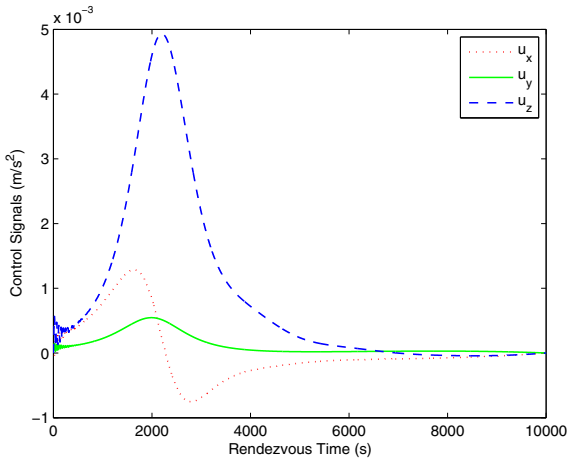

Fig. 3. Control signals of the chaser spacecraft

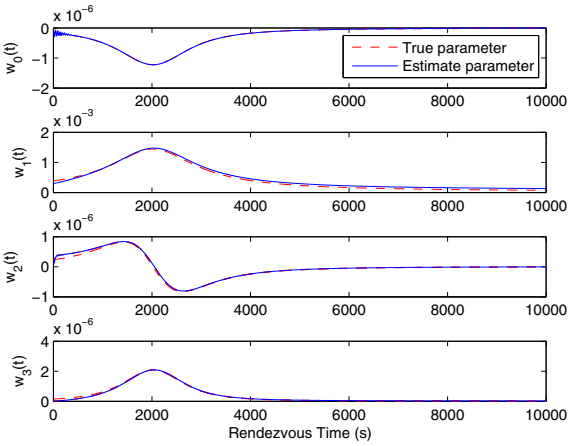

Fig. 4. Estimate parameter curves

values. Then, the elliptical orbit of target spacecraft is determined.

Table 2. Calculated orbital elements

Orbital elements	Calculated value
Eccentricity	0.691
Semimajor (km)	22863
Time of perigee passage (s)	2103

6. CONCLUSION

In this paper, we present a strategy which can not only control autonomous rendezvous but also estimate the orbital elements. An example of rendezvous motion is provided to show the implementation of the control and estimation methods. The simulation results show that the actual trajectories track the reference trajectories tightly, and the estimated orbital elements can determine the target orbit.

REFERENCES

Gao, X., Teo, K.L., and Duan, G.R. (2012). Robust H_∞ control of spacecraft rendezvous on elliptical orbit. *Journal of the Franklin Institute*, 349, 2515–2529.

Han, J. (2009). From PID to active disturbance rejection control. *IEEE Transactions on Industrial Electronics*, 56(3), 900–906.

Hang, C. and Guo, L. (2012). Control of a class of nonlinear uncertain systems by combining state observers and parameter estimators. In *Proceedings of the 10th World Congress on Intelligent Control and Automation*, 2054–2059.

Inalhan, G., Tillerson, M., and How, J.P. (2002). Relative dynamics and control of spacecraft formations in eccentric orbits. *Journal of Guidance, Control, and Dynamics*, 25(1), 48–59.

Karlgaard, C.D. and Schaub, H. (2011). Adaptive nonlinear Huber-based navigation for rendezvous in elliptical orbit. *Journal of Guidance, Control, and Dynamics*, 34(2), 388–402.

Khalil, H. (2002). *Nonlinear Systems*. Prentice Hall, New Jersey.

Lu, S. and Xu, S. (2009). Adaptive control for autonomous rendezvous of spacecraft on elliptical orbit. *Acta Mechanica Sinica*, 25(1), 539–545.

Simon, D. (2006). *Optimal State Estimation: Kalman, H_∞, and Nonlinear Approaches*. Wiley, New Jersey.

Singla, P. and Subbarao, K. (2008). Stable adaptive reference trajectory modification for saturated control applications. In *Proceedings of the 2008 American Control Conference*, 3470–3475.

Singla, P., Subbarao, K., and Junkins, J.L. (2006). Adaptive output feedback control for spacecraft rendezvous and docking under measurement uncertainty. *Journal of Guidance, Control, and Dynamics*, 29(4), 892–902.

Westervelt, E.R., Grizzle, J.W., Chevallereau, C., Choi, J.H., and Morris, B. (2007). *Feedback control of dynamic bipedal robot locomotion*. CRC press, New York.

Wong, H., Kapila, V., and Sparks, A.G. (2002). Adaptive output feedback tracking control of spacecraft formation. *International Journal of Robust and Nonlinear Control*, 12(2-3), 117–139.

Wu, H., Hu, J., and Xie, Y. (2007). Characteristic model-based all-coefficient adaptive control method and its applications. *IEEE Transactions on Systems, Man, and Cybernetics, Part C: Applications and Reviews*, 37(2), 213–221.

Xie, Y., Hu, J., Wang, M., Hu, H., and Zhang, H. (2013). Accurate and stable control of shenzhou spacecraft in rendezvous and docking. In *Proceedings of the 19th IFAC symposium on automatic control in aerospace*, 524–528.

Xue, W. and Huang, Y. (2011). Comparison of the DOB based control, a special kind of PID control and ADRC. In *Proceedings of the 2011 American Control Conference*, 4373–4379.

Yamanaka, K. and Ankersen, F. (2002). New state transition matrix for relative motion on an arbitrary elliptical orbit. *Journal of Guidance, Control, and Dynamics*, 25(1), 60–66.

Yucelen, T. and Calise, A.J. (2011). Derivative-free model reference adaptive control. *Journal of Guidance, Control, and Dynamics*, 34(4), 933–950.

Zhou, B., Lin, Z., and Duan, G.R. (2011). Lyapunov differential equation approach to elliptical orbital rendezvous with constrained controls. *Journal of Guidance, Control, and Dynamics*, 34(2), 345–358.